

Supporting Information

Title: Quasi Talbot effect of orbital angular momentum beams for generation of optical vortex arrays by multiplexing metasurface design

Hui Gao, Yang Li, Lianwei Chen, Jinjin Jin, Mingbo Pu, Xiong Li, Ping Gao, Changtao Wang, Xiangang Luo and Minghui Hong

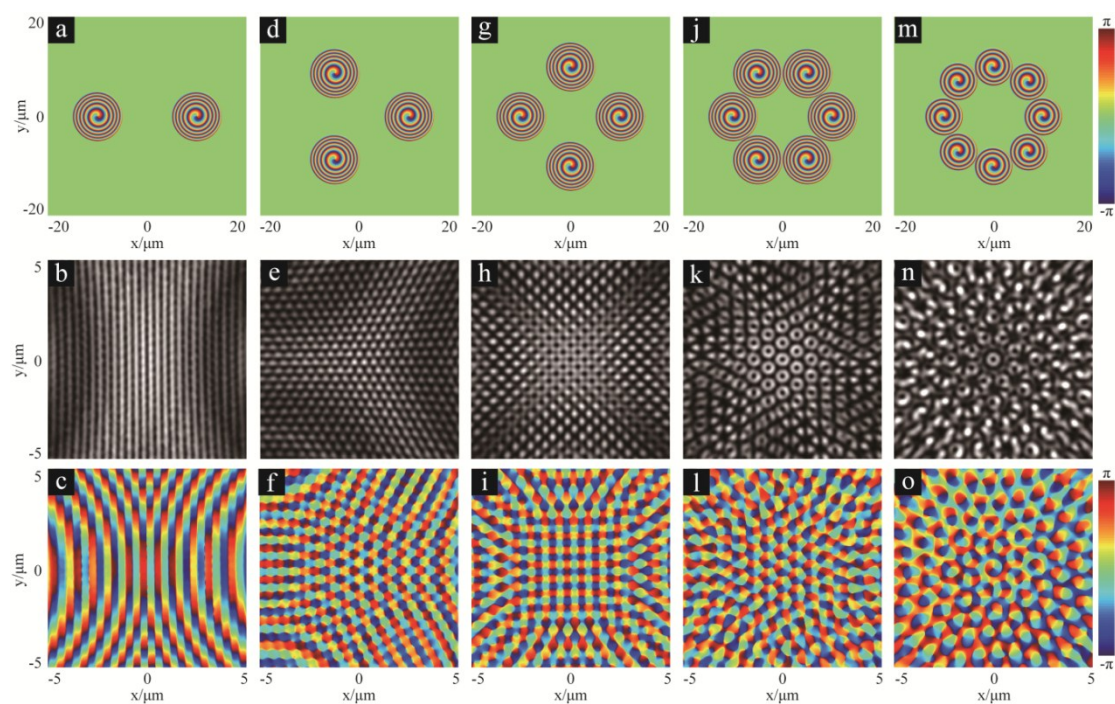


Figure S1. Simulation results of interference on defocusing plane with different amount of OAM lenses. Illustrations in the first line (a, d, g, j, and m) are phase maps of metasurface samples, the amounts of OAM lenses are 2, 3, 4, 6 and 8, separately. These centers of OAM lenses with same topological charges $l=1$ and same focal lengths $f=5\mu\text{m}$ are placed at the vertex points of corresponding regular polygons, and the circumcircle radiuses of these regular polygons are same $d=10\mu\text{m}$ (when the amount of OAM lenses is 2, they are placed away with each other at distance $20\mu\text{m}$). Illustrations in the second line (b, e, h, k, and n) are corresponding intensity distribution of interference results on defocusing plane. The distance between focal plane and the defocusing plane is $D=15\mu\text{m}$. Illustrations in the third line (c, f, i, l, and o) are corresponding phase distribution of interference results on defocusing plane.

To get vortex beam arrays in gapless arrangement with good hollow shape, parameters are optimized with the numerical calculation by vector diffraction theory. It is found that keeping good symmetry is helpful to satisfy the phase matching of quasi Talbot effect to generate vortex beam arrays. The centers of these OAM lenses are placed at the vertex points of corresponding regular polygons to improve symmetry, and the sizes of the circumcircles of these regular polygons are limited by fabrication capability. The radius of circumcircle in our design is $d=10\mu\text{m}$ as shown in

Figure S1 because the size of fabrication area of FIB in our experiment is $30\mu\text{m}\times 30\mu\text{m}$. Meanwhile, the performance of multiplexing is related to the size of single OAM lens which means that the amounts of OAM lenses cannot be a large number. So the maximum of the amount is set as 8 in the simulation.

The interference results of two OAM lenses in Figure S1(a) is parallel lines distribution in central zone as shown in Figure S1(b). When the amount of OAM lenses is an even number (such as 4, 6 and 8), the symmetry is well enough to generate OAM arrays as shown in Figures S1 (h),(k),(n). But if the amount of OAM lenses is an odd number (for example, 3), there are point arrays on defocusing plane because symmetry and phase matching is broken as shown in Figure S1(e). To achieve gapless arrangement and good shape of vortex arrays, the best choice about the amount of OAM lenses is found to be 6.

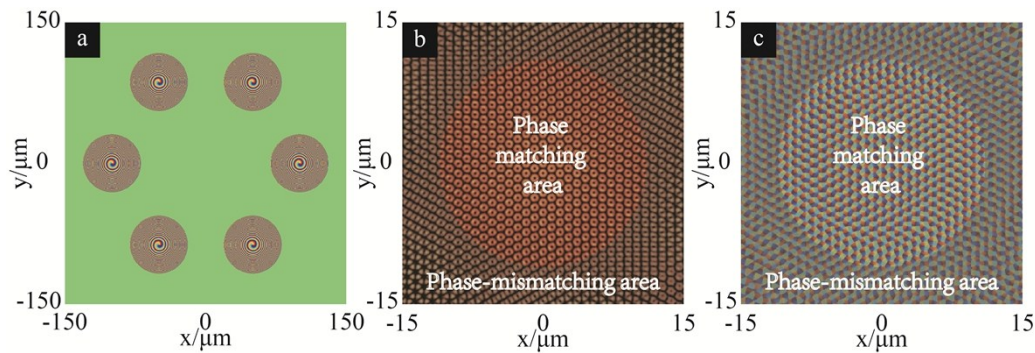


Figure S2. Simulation results of interference on defocusing plane with parameters as follow: $l=1$, $N=6$, $d=100\mu\text{m}$, $f=50\mu\text{m}$, $D=200\mu\text{m}$. (a) The phase map of device. (b) The intensity distribution of interference results on defocusing plane. (c) The phase distribution of interference results on defocusing plane.

As explained in report, the size of self-imaging area and multiplication factor are related to parameter d to satisfy the phase matching in this quasi Talbot effect. In our experiment, $d=10\mu\text{m}$ is small because of fabrication limitation and the multiplication factor is also not a large number. But the multiplication factor can be increased easily by enlarging the sample size. For example, Figure S2 shows the self-imaging result when $N=6$ and $d=100\mu\text{m}$. There are more than 360 optical vortexes in central phase-matching area which means the multiplication factor is more than 60.

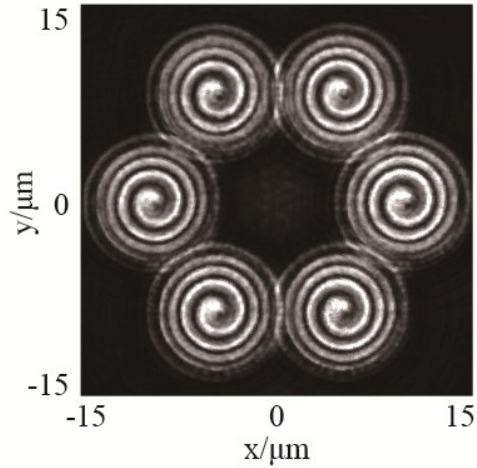


Figure S3. Interference result of planar wave and OAM lenses' light field. By illuminating the device in Figure 3 with linear polarized laser, converted light fields by OAM lenses interfere with the non-converted planar wave and generate helical light field with single spiral arm which implies the topological charge $l=1$.

To ensure the topological charges of OAM lenses in our experiment, the metasurface device is illuminated by linear polarized laser. The converted light fields by OAM lenses interfere with the non-converted planar wave and generate helical light field with single spiral arm which implies the topological charge $l=1$ as shown in Fig. S3.

As authors have declared that there's no rotation among N OAM lenses while their centres are placed at vertex positions of a regular polygon separately in our design (Page 2 in main body of paper). We numerically simulated the interference results of 6 OAM lenses w/ and w/o rotation in Fig. S4. Also to clarify the difference between conventional N -beam interference and vortex beam interference, we calculated the phase and intensity distributions of interference results of 6 meta-lenses. The design in Column 1 (first column) of Fig. S4 is same with that in Fig. 3 of main body. Column 2 shows the design with rotation of each OAM lens, and n th OAM lens rotates $n \cdot 360/N$ degree, where $n=1,2,\dots,N$. Column 3 presents the interference results of 6 meta-lens with same focal length.

The phase maps of three different designs are shown in Row a (first row) of Fig. S4. And intensity distributions on the defocusing planes are presented in Row b while light fields distributions on zoomed in area of interest are mapped in Row c of Fig. S4. The figures of Row d are phase map corresponding to Row c. From the column 2, it can be seen that the rotation of $n \cdot 360/N$ degree for n th OAM lens offset the vortex phase in Column 1.

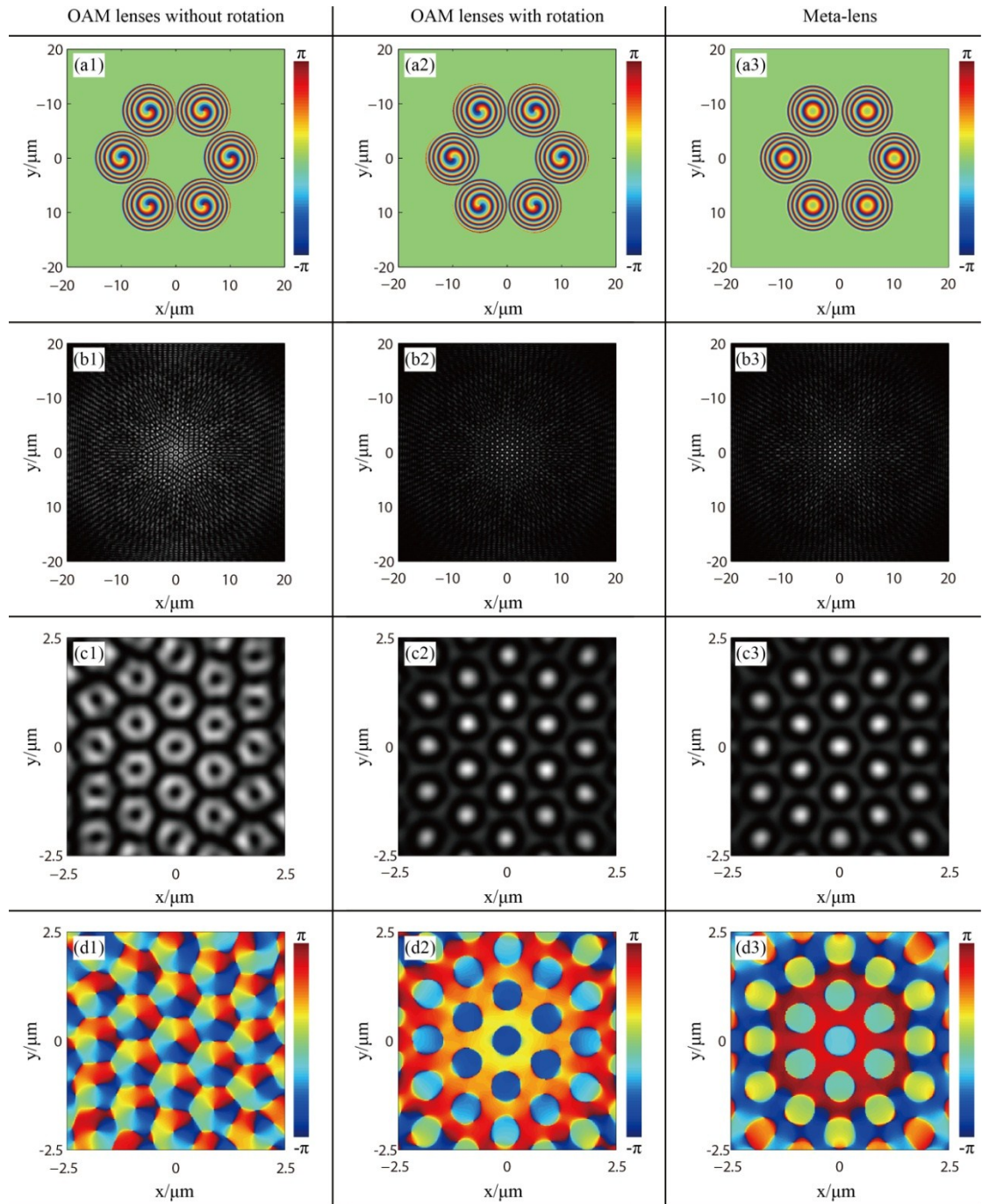


Figure S4. The comparisons of three kinds of different designs. Column 1: 6 OAM lenses w/o rotation. Column 2: 6 OAM lenses w/ rotation of $n \cdot 360/N$ degree for n th OAM lens. Column 3: 6 meta-lenses. Row a: phase distributions of samples. Row b: intensity distributions on the defocusing planes. Row c: light fields distributions on zoomed in area of interest. Row d: phase map corresponding to Row c.